LAWRENCE
LIVERMORE
NATIONAL
LABORATORY

UCRL-JRNL-223906

QED Corrections to the 4p - 4d Transition Energies of Copperlike Heavy Ions

M. H. Chen, K. T. Cheng, W. R. Johnson, J. Sapirstein

August 23, 2006

Physical Review A

QED corrections to the $4p - 4d$ transition energies of copperlike heavy ions

M. H. Chen* and K. T. Cheng†

University of California, Lawrence Livermore National Laboratory, Livermore, CA 94550

W. R. Johnson‡ and J. Sapirstein§

Department of Physics, University of Notre Dame, Notre Dame, IN 46556

(Dated: August 21, 2006)

Abstract

Quantum electrodynamic (QED) corrections to $4p - 4d$ transition energies of several copperlike ions with $Z = 70 - 92$ are calculated non-perturbatively in strong external fields to all orders in binding corrections. Dirac-Kohn-Sham potentials are used to account for screening and core-relaxation effects. For the $4p_{1/2} - 4d_{3/2}$ transition in copperlike bismuth, thorium and uranium, results are in good agreement with empirical QED corrections deduced from differences between transition energies obtained from recent high-precision electron-beam ion-trap (EBIT) measurements and those calculated with the relativistic many-body perturbation theory (RMBPT). These comparisons provide sensitive tests of QED corrections for high angular momentum states in many-electron heavy ions and illustrate the importance of core-relaxation corrections. Comparisons are also made with other theories and with experiment on the $4s - 4p$ transition energies of high-Z Cu-like ions as accuracy checks of the present RMBPT and QED calculations.

PACS numbers: 31.30.Jv, 32.30.Rj, 31.25.-v, 31.15.Ar

*chen7@llnl.gov

†ktcheng@llnl.gov

‡johnson@nd.edu

§jsapirst@nd.edu

I. INTRODUCTION

Quantum electrodynamic (QED) corrections to binding energies of electrons in strong nuclear fields have been the subject of many studies in the past. Of particular interests are QED corrections in high-Z, many-electron ions where screening corrections to the self-energy and vacuum polarization are important [1, 2]. Advances in theory and experiment have reached such high accuracy that even small contributions from the two-loop Lamb shift can now be tested [2, 3]. However, most of the existing works deal with $ns - np$ transitions and very few, if any, precision tests are available for higher angular momentum states. While QED corrections are expected to be small for high-l bound electron as the centrifugal barrier $l(l+1)/2r^2$ prevents them from getting too close to the nucleus, their contributions may not be negligible for heavy ions and should be included when comparing theory with high-precision spectroscopic measurements. Such is the case with the recent electron-beam ion-trap (EBIT) measurements which have produced highly-accurate x-ray energies for the $4p_{1/2} - 4d_{3/2}$ transition in copperlike bismuth, thorium and uranium [4]. With transition energies measured at 366.72(2), 491.94(10) and 535.15(5) eV, respectively, results are sensitive enough to test QED corrections, estimated at -0.24, -0.48 and -0.54 eV [5], to about the 10% level. Before such tests can be carried out, however, atomic transition energy calculations must reach a comparable level of accuracy. Early theoretical calculations for Cu-like ions are based mostly on the multiconfiguration Dirac-Fock (MCDF) method [6, 7] which is accurate to about 1 eV, enough to reveal QED contributions to the $4s - 4p$ transitions which are about $2 - 3$ eV in size, but not enough to reveal those to the $4p - 4d$ transitions which are one order of magnitude smaller. With advances in relativistic correlation calculations such as the relativistic many-body perturbation theory (RMBPT) [8] and the relativistic configuration-interaction (RCI) method [9], atomic correlation energies can now be calculated very accurately, paving the way for precision tests of small QED corrections from high-l states of Cu-like heavy ions.

The most sophisticated relativistic correlation calculations for the copper isoelectronic sequence were carried out by Johnson *et al.* [8] with RMBPT to third order in both Coulomb and Breit interactions. Large-scale RCI calculations have also been carried out recently by Cheng and Chen [9] with comparable accuracy. As for QED corrections, Kim *et al.* [10] have calculated QED energies by adjusting hydrogenic values with the Welton method to

account for screening corrections. *Ab initio* S-matrix calculations have also been carried out by Blundell [11], who evaluated the one-loop self-energy and vacuum polarization diagrams directly, along with dominant screening and relaxation corrections from higher-order correlation diagrams. QED energies similar to the ones shown in the following have also been given by Cheng and Chen [9]. In all of these correlation and QED calculations, however, only $4s-4p$ transitions are considered. Recently, Sapirstein and Cheng [5] calculated QED corrections for Cu-like $4d$ states using Dirac-Kohn-Sham (DKS) potentials to account for screening corrections. They showed that their QED corrections to the $4p_{1/2}-4d_{3/2}$ transition are consistent with those inferred from the EBIT measurements [4]. However, no detailed comparisons between theory and experiment have been carried out so far.

In this work, relativistic correlation energies for the $4p-4d$ transitions in Cu-like ions with $Z = 70$, 74, 76, 79, 82, 83, 90 and 92 are calculated with RMBPT, while QED energies are calculated with DKS potentials in Furry's bound-interaction representation [12] to account for screening and relaxation effects. Results for the $4s-4p$ transitions are also presented here to provide checks on the accuracy of our calculations. The present QED results are in good agreement with available empirical QED corrections deduced from differences between the measured and the RMBPT energies. In particular, it is shown that for the $4p_{1/2}-4d_{3/2}$ transition, core-relaxation corrections are large and are instrumental in bringing good agreement between theory and experiment. In the following section, the present RMBPT and QED calculations are described. In section III, our results are presented and compared with other theories and with experiment. Finally, in section IV, we summarize our findings.

II. THEORETICAL CALCULATIONS

Details of the RMBPT calculations were given in Ref. [8]. Here, we briefly outline the essential features. Our RMBPT calculations are based on the *no-pair* Hamiltonian [13–15] which includes Coulomb and frequency-dependent Breit interactions. To facilitate sums over intermediate states, single-particle basis orbitals for the Dirac equation are obtained from an expansion in terms of B-splines [16]. The perturbation expansion is carried out through third order for both the Coulomb and Breit correlation corrections. Fourth-order Coulomb correlation corrections were studied in [8] and found to be smaller than the numerical error

for copper-like ions with $Z > 50$. Mass-polarization corrections were included perturbatively through third order with the operator $\frac{1}{M}\sum_{i<j}\mathbf{p}_i \cdot \mathbf{p}_j$. Their contributions are found to be consistently less than 0.01 eV and are not shown here. Nuclear finite size effects are also included, with parameters for the Fermi charge distribution of the nucleus taken from Johnson and Soff [17], except for thorium and uranium which are from Zumbro *et al.* [18, 19].

In this work, QED corrections are calculated from the one-loop self-energy and vacuum polarization diagrams shown in Fig. 1. Electron self-energies are calculated non-perturbatively in the external potential with partial wave expansions in configuration space. Subtraction terms involving the free-electron propagator are evaluated in momentum space, which requires accurate Fourier-transformed wave functions. Details of our self-energy calculations, with references to earlier works, can be found in Ref. [5]. As for vacuum polarization, leading contributions are obtained from expectation values of the Uehling potential, while higher-order Wichmann-Kroll corrections, like the self-energies, are calculated non-perturbatively in the external potential with partial wave expansions in the configuration space using the method of Sapirstein and Cheng [20].

For many-electron systems such as Cu-like ions, correlation corrections to the one-loop radiative diagrams are significant. Examples of these radiative correlation diagrams are shown in Fig. 2. As pointed out by Blundell [1], screening corrections to the valence electron from direct-interaction diagrams such as those shown in Figs. 2(a) – 2(d) can be accounted for exactly by evaluating the one-loop diagrams with a "core-Hartree" potential $V(r)$ such that

$$V(r) = V_{\rm C}(r) + e^2 \int_0^r dr' \frac{1}{r_>}\rho(r'), \tag{1}$$

where $V_{\rm C}(r) = -Ze^2/r$ is the nuclear potential and $\rho(r)$ is the radial charge density of the Ni-like core

$$\rho(r) = \sum_c (2j_c + 1)\rho_c(r). \tag{2}$$

In particular, $\rho_c(r) = g_c^2(r) + f_c^2(r)$ is the radial charge density of a core electron c and $g_c(r)$ and $f_c(r)$ are the upper and lower components of the radial Dirac wave functions determined self-consistently by the Dirac-Hartree equation. Likewise, a core electron can be screened by other core electrons as well as by the valence electron in a "modified core-Hartree" potential with the charge density

$$\rho(r) = \rho_v(r) + {\sum_c}' (2j_c + 1)\rho_c(r), \tag{3}$$

where v and c refer to valence and core electrons, respectively, and the sum $\sum'$ goes over one less core electron from the same subshell. Core screening diagrams are the same as those shown in Figs. 2(a) – 2(d), but with the core- and valence-electron indices "c" and "v" interchanged. Blundell further calculated exchange-interaction "side" diagrams such as those shown in Figs. 2(e) and 2(g) as one-loop diagrams with perturbed orbitals, but exchange-interaction "vertex" diagrams such as those shown in Figs. 2(f) and 2(h) were neglected with the expectation that their contributions should be small.

In this work, one-loop radiative diagrams are evaluated with N-electron Dirac-Kohn-Sham potentials instead of $(N-1)$-electron core-Hartree or modified core-Hartree potentials. This is equivalent to using the total charge density of the atomic state

$$\rho(r) = \rho_v(r) + \sum_c (2j_c + 1)\rho_c(r) \tag{4}$$

and adding to $V(r)$ an average exchange potential

$$V_{\rm ex} = -x_\alpha \frac{e^2}{r} \left[\frac{81}{32\pi^2}\, r\, \rho(r)\right]^{1/3}. \tag{5}$$

In particular, $x_\alpha = 0$, 2/3 and 1 for Hartree, Kohn-Sham and Slater averaged-exchange potentials, respectively. With $N-$electron DKS potentials, self-interaction contributions will not cancel exactly between the direct- and exchange-interaction diagrams, but these residual corrections should be quite small. Computationally, they have the advantage over core-Hartree and modified core-Hartree potentials in that the same screening potential is used for QED calculations of all electrons in an atomic state. Once one-electron QED energies ϵ_i are calculated for each subshell i, total QED correction to the energy level is given by

$$E_{\rm QED} = \epsilon_v + \sum_c (2j_c + 1)\epsilon_c. \tag{6}$$

In a "frozen-core" approximation where the same potential is used to calculate the ϵ's for both the initial and final states, QED corrections to transition energies are simply given by differences in ϵ_v's. To account for relaxation corrections, we use DKS potentials specific to the initial- and final-state valence configurations. This leads to slightly different one-electron QED energies for the same atomic subshells in the initial and final states, and core-electron contributions no longer cancel exactly. As we shall show in the following, these core-relaxation corrections are very important for the $4p_{1/2} - 4d_{3/2}$ transition.

It should be noted that QED corrections thus calculated will be potential dependent and the key is to choose model potentials that minimize contributions from higher-order correlation diagrams. DKS potentials are used here because they have been shown to give very accurate QED energies for the $2s-2p$ transitions in high-Z Li- and Be-like ions [21], the $3s-3p$ transitions in Na-like to Al-like uranium [22], and the $4s-4p$ transition in heavy Cu-like ions [9]. They should work just as well for the $4p-4d$ transitions here.

In this work, two-loop Lamb shifts of the $4s$ electrons are inferred from known values of the $1s$ states of H-like ions [23] by screening estimates and $1/n^3$ scalings. For the $4p$ and $4d$ electrons, we assume that two-loop contributions are negligible.

III. RESULTS AND DISCUSSION

Tables I and II shows typical QED results for high-Z Cu-like ions using Cu-like uranium as an example. In Table I, QED energies from $1s$ to $4d$ states are shown. DKS potentials $V(4l)$ with the same $3d^{10}$ Ni-like core but different $4l$ valence electrons are used in these calculations. In most cases, changes in QED energies from different DKS potentials are much less than 0.1% and are hardly noticeable except for the self-energies and Uehling potential terms of inner core electrons. Changes in Wichmann-Kroll contributions are consistently quite negligible.

From Eq. (6), QED corrections to $4l-4l'$ transition energies are given by

$$\Delta E_{\rm QED} = (\epsilon'_{4l'} - \epsilon_{4l}) + \sum_c (2j_c+1)(\epsilon'_c - \epsilon_c) = \Delta E_{\rm valence} + \Delta E_{\rm relax}, \tag{7}$$

where ϵ and ϵ' are one-electron QED energies calculated in DKS potentials of the initial $3d^{10}4l$ and final $3d^{10}4l'$ states, respectively,

$$\Delta E_{\rm valence} = \epsilon_{4l'} - \epsilon_{4l} \tag{8}$$

are leading contributions from the valence electrons in a frozen-core approximation, and

$$\Delta E_{\rm relax} = (\epsilon'_{4l'} - \epsilon_{4l'}) + \sum_c (2j_c+1)(\epsilon'_c - \epsilon_c), \tag{9}$$

are relaxation corrections. From Table I, it is clear that valence contributions to relaxation corrections from the first term in Eq. (9) are negligible and that $\Delta E_{\rm relax}$ are dominated by core-relaxation corrections from the second term which can be sizeable, especially after summing contributions from all 28 core electrons.

Table II shows QED corrections to the $4s-4p$ and $4p-4d$ transition energies of Cu-like uranium. Shell-by-shell contributions from the $1s$ to $3d$ core states, weighted by the number of electrons in the subshell, are shown. Resulting core-relaxation corrections $\Delta E_{\rm relax}$ are small compared to valence-electron contributions $\Delta E_{\rm valence}$. However, for the $4p_{1/2}-4d_{3/2}$ transition, the core-relaxation correction is surprising large at close to 0.08 eV, and amounts to a 14% correction to the -0.58 eV total QED correction. In contrast, core-relaxation corrections for the $4s-4p_{1/2}$ and $4s-4p_{3/2}$ transitions are smaller at -0.02 and 0.03 eV, respectively, and amount to less than 1% of the respective QED corrections.

To check the accuracy of our core-relaxation calculations which depend on large cancellations between the one-electron QED energies ϵ_c and ϵ_c', we have carried out similar QED calculations with Dirac-Slater instead of Dirac-Kohn-Sham potentials. Core-relaxation results are found to be essentially the same and are thus unlikely to be affected much by numerical cancellations. At the same time, QED energies change by as much as 0.08 eV for the $4s-4p$ transitions and about 0.02 eV for the $4p-4d$ transitions, underscoring the potential dependence of our QED calculations. But as mentioned earlier, DKS potentials are used here because they have been shown to give very good QED energies in the past. Our results shown in the following will give further support to these choices.

In Table III, Coulomb and Breit contributions to the RMBPT energies are shown for the $4s-4p$ transitions in Cu-like ions with $Z=70$, 74, 76, 79, 82, 83, 90 and 92. Mass polarization contributions are consistently very small and are not listed here. It can be seen that the present RMBPT energies, with improved numerical calculations, differ slightly from previous RMBPT results [8] and consistently agree with RCI energies [9] to better than 0.02 eV. We thus take 0.02 eV as the estimated uncertainty of the present RMBPT energies. In the same table, QED corrections to the $4s-4p$ transition energies are also shown. The main uncertainty in our QED results should come from residual correlation corrections not accounted for by the DKS potentials, and are estimated to be about 0.04 eV. Our total energies, shown with root-mean-square errors from RMBPT and QED, are in very good agreement with recent high-precision dielectronic recombination [24] and EBIT [4, 25, 26] measurements. We note that detailed comparisons between theory and experiment for the $4s-4p$ transitions have been given in Ref. [9] before, with RCI instead of RMBPT but the same QED energies. Here, comparisons are extended to include more Cu-like ions ($Z=70$, 76 and 83) where high-precision measurements are also available.

In Table IV, RMBPT, QED and total energies of the $4p - 4d$ transitions are shown. Again, mass polarization contributions are small and are not shown. Likewise, two-loop Lamb shift contributions to the QED energies are omitted here. To our knowledge, no other theoretical results on atomic transition energies or QED corrections are available for comparisons, but our $4p-4d$ results should be of comparable accuracy as our $4s-4p$ results. Indeed, the only experimental data available are for the $4p_{1/2} - 4d_{3/2}$ transition in Cu-like bismuth, thorium and uranium [4] and our total transition energies do agree with these data to within experimental uncertainties. While QED energies for the $4p - 4d$ transitions are much smaller than those for the $4s - 4p$ transition, they are still one order of magnitude larger than the experimental errors and are definitely not negligible.

Table V shows empirical QED energies as deduced from the measured data by subtracting the RMBPT transition energies, with root-mean-square errors from RMBPT and experimental uncertainties. They are compared with the present QED results calculated with and without core-relaxation corrections. For the $4s - 4p$ transitions, Blundell's QED energies [11] from S-matrix calculations of dominant QED correlation diagrams are also presented, along with those by Kim *et al.* [10] which are scaled from hydrogenic results with the *ad hoc* Welton's method. Comparisons of these results are shown graphically in Figs. 3 – 5, where QED energies scaled by $(Z\alpha)^4$ are plotted as functions of the nuclear charge Z for the $4s_{1/2} - 4p_{1/2}$, $4s_{1/2} - 4p_{3/2}$ and $4p_{1/2} - 4d_{3/2}$ transitions, respectively. It can be seen that our QED energies are in good agreement with Blundell's results and with empirical data, but deviate from those of Kim *et al.*, especially at high Z. Also, while core-relaxation corrections slightly worsen the agreement of our QED energies with Blundell's and empirical results for the $4s - 4p_{1/2}$ transition, they improve the agreement for the $4s - 4p_{3/2}$ and $4p_{1/2} - 4d_{3/2}$ transitions. With these corrections included, our QED energies are *consistently* below the empirical data for all three transitions, and these residual discrepancies are likely due to uncalculated higher-order radiative correlation diagrams. While core relaxation corrections are relatively insignificant for $4s - 4p$ transitions and amount to less than 1% corrections to the QED energies, they are substantial corrections for $4p - 4d$ transitions and amount to 32% – 14% corrections for $Z = 70 - 92$ in the case of $4p_{1/2} - 4d_{3/2}$ transition. From Fig. 5, it is clear that these corrections, which are up to twice as big as the errors of the empirical data, are important in bringing theory into agreement with experiment.

IV. SUMMARY

In this paper, we have calculated the $4s-4p$ and $4p-4d$ transition energies for copperlike ions with Z = 70, 74, 76, 79, 82, 83, 90, and 92. Our results include relativistic correlation energies calculated with RMBPT and screened QED corrections calculated with DKS model potentials. Good agreement between theory and recent high-precision measurements are found. In particular, core-relaxation corrections to QED energies, which are relatively unimportant for the $4s-4p$ transitions, are found to be quite significant for the $4p_{1/2}-4d_{3/2}$ transition. Further improvement in theory will come from direct evaluations of the complete set of radiative correlation diagrams such as the calculations shown in Ref. [2]. It is worth noting that the much simpler approach here can readily give results close to the accuracy of the best available measurements and can be used as a starting point for more rigorous QED calculations.

Acknowledgments

The work of M.H.C and K.T.C. was performed under the auspices of the U.S. Department of Energy by the University of California, Lawrence Livermore National Laboratory under Contract No. W-7405-ENG-48. The work of W.R.J. was supported in part by NSF Grant No. PHY-0456828. The work of J.S. was supported in part by NSF Grant No. PHY-0451842.

[1] S. A. Blundell, Phys. Rev. A **46**, 3762 (1992).

[2] J. Sapirstein and K. T. Cheng, Phys. Rev. A **64**, 022502 (2001).

[3] P. Beiersdorfer, H. Chen, D. B. Thorn, and E. Träbert, Phys. Rev. Lett. **95**, 233003 (2005).

[4] E. Träbert, P. Beiersdorfer, K. B. Fourier and M. H. Chen, Can. J. Phys., **82**, 1 (2004).

[5] J. Sapirstein and K. T. Cheng, Phys. Rev. A **73**, 012503 (2006).

[6] J. F. Seely, J. O. Ekberg, C. M. Brown, U. Feldman, W. E. Behring, J. Reader, and M. C. Richardson, Phys. Rev. Lett. **57**, 2924 (1986).

[7] K. T. Cheng and R. A. Wagner, Phys. Rev. A **36**, 5435 (1987).

[8] W. R. Johnson, S. A. Blundell, and J. Sapirstein, Phys. Rev. A **42**, 1087 (1990).

[9] K. T. Cheng and M. H. Chen, Radiation Physics and Chemistry, in press.

[10] Y.-K. Kim, D. H. Baik, P. Indelicato, and J. P. Desclaux, Phys. Rev. A **44**, 148 (1991).

[11] S. A. Blundell, Phys. Rev. A **47**, 1790 (1993).

[12] W. H. Furry, Phys. Rev. **81**, 115 (1951).

[13] G. E. Brown and D. G. Ravenhall, Proc. R. Soc. London, Ser. A **208**, 552 (1951).

[14] J. Sucher, Phys. Rev. A **22**, 348 (1980).

[15] M. H. Mittleman, Phys. Rev. A **4**, 893 (1971); **5**, 2395 (1972); **24**, 1167 (1981).

[16] W. R. Johnson, S. A. Blundell, and J. Sapirstein, Phys. Rev. A **37**, 307 (1988).

[17] W. R. Johnson and G. Soff, At. Data Nucl. Data Tables, **33**, 405 (1985).

[18] J. D. Zumbro, R. A. Naumann, M. V. Hoehn, E. B. Shera, C. E. Bemis, Jr., and Y. Tanaka, Phys. Lett. **167B**, 383 (1986).

[19] J. D. Zumbro, E. B. Shera, Y. Tanaka, C. E. Bemis, Jr., R. A. Naumann, M. V. Hoehn, W. Reuter, and R. M. Steffen, Phys. Rev. Lett. **53**, 1888 (1984).

[20] J. Sapirstein and K. T. Cheng, Phys. Rev. A **68**, 042111 (2003).

[21] K. T. Cheng, M. H. Chen, and J. Sapirstein, Phys. Rev. A **62**, 054501 (2000).

[22] M. H. Chen, K. T. Cheng, P. Beiersdorfer, and J. Sapirstein, Phys. Rev. A **68**, 022507 (2003).

[23] V. A. Yerokhin, P. Indelicato and V. M. Shabaev, Eur. Phys. J. D **25**, 203 (2003).

[24] E. Lindroth, H. Danared, P. Glans, Z. Pešić, M. Tokman, G. Vikor, and R. Schuch, Phys. Rev. Lett. **86**, 5027 (2001).

[25] S. B. Utter, P. Beiersdorfer, E. Träbert and E. J. Clothiaux, Phys. Rev. A **67**, 032502 (2003).

[26] E. Träbert, P. Beiersdorfer, and H. Chen, Phys. Rev. A, **70**, 032506 (2004).

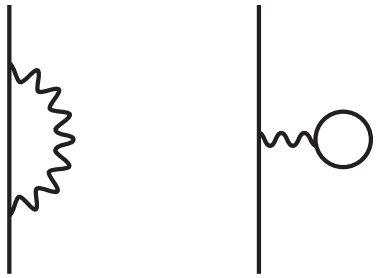

FIG. 1: One-loop self-energy and vacuum polarization diagrams.

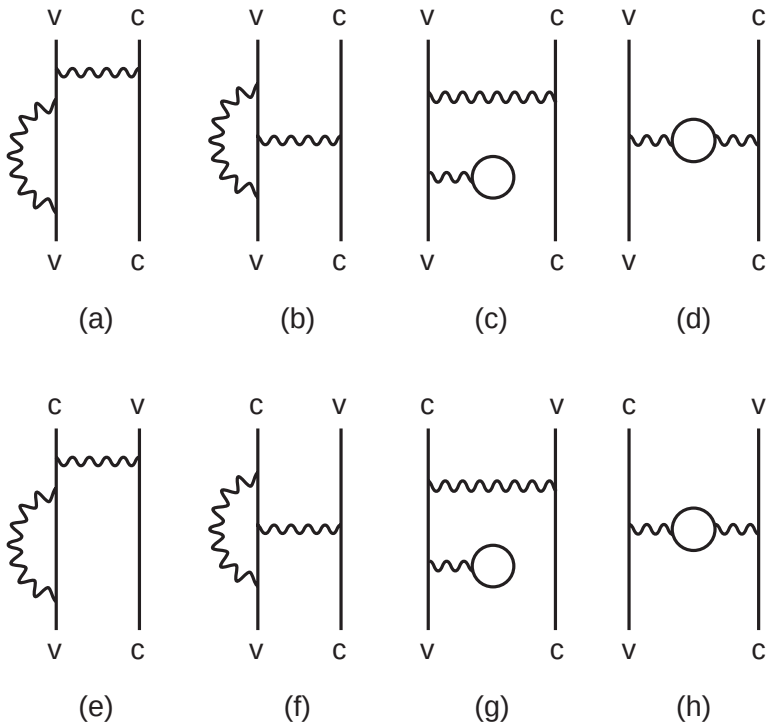

FIG. 2: Typical radiative correlation diagrams.

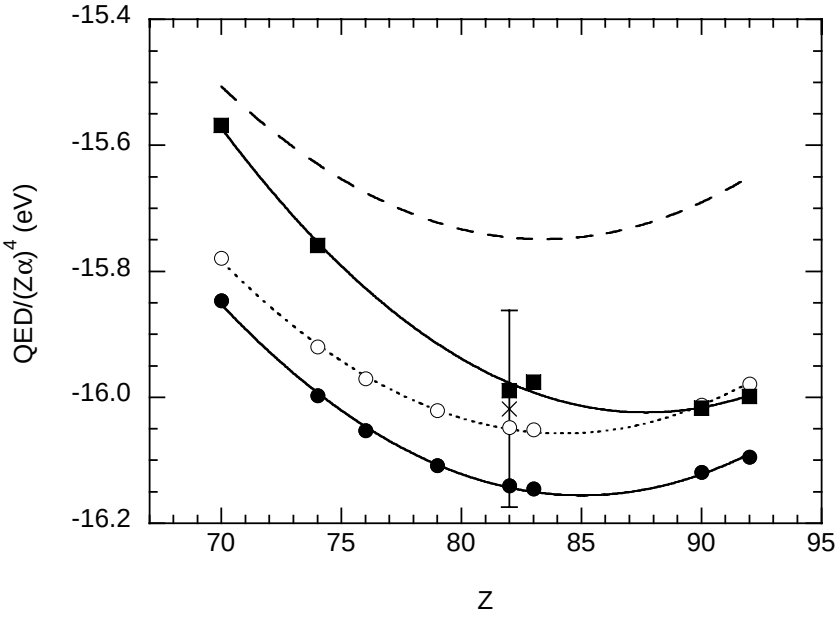

FIG. 3: Scaled QED energies for the $4s - 4p_{1/2}$ transitions. Open and closed circles are frozen-core and relaxed-core results of this work, solid squares are Blundell's results [11], the dashed line shows results of Kim *et al.* [10], and the cross with an error bar is the empirical data.

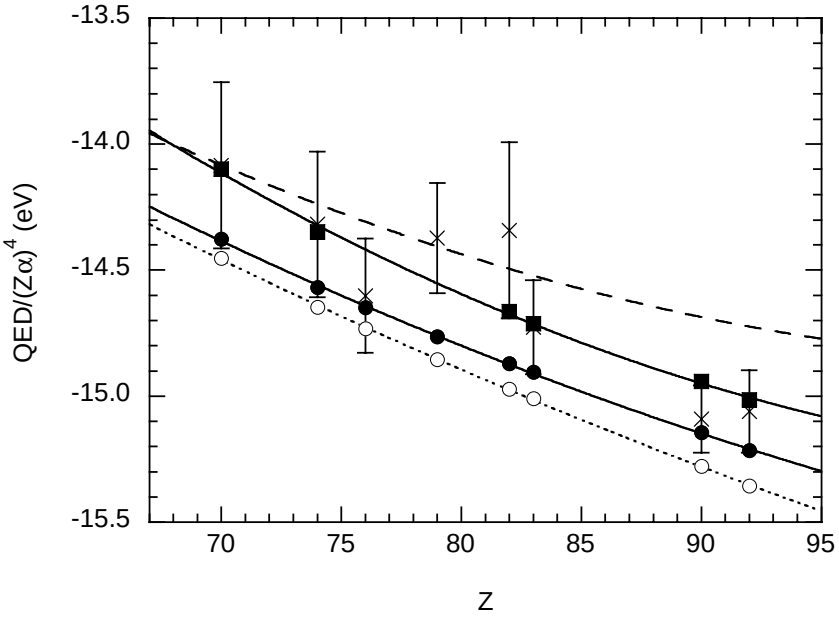

FIG. 4: Scaled QED energies for the $4s - 4p_{3/2}$ transitions. Open and closed circles are frozen-core and relaxed-core results of this work, solid squares are Blundell's results [11], the dashed line shows results of Kim *et al.* [10], and crosses with error bars are empirical data.

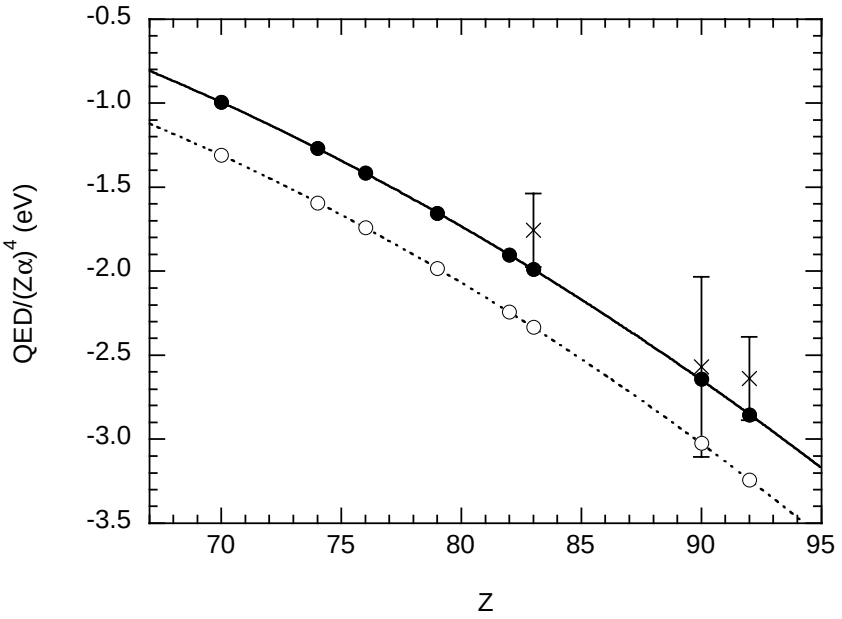

FIG. 5: Scaled QED energies for the $4p_{1/2} - 4d_{3/2}$ transitions. Open and closed circles are frozen-core and relaxed-core results of this work, and crosses with error bars are empirical data.

TABLE I: One-electron self-energy (SE), Uehling potential (UP), Wichmann-Kroll (WK) and QED energies (eV) of Cu-like uranium as calculated in DKS potentials $V(4l)$ with $3d^{10}4l$ configurations.

State	$V(4s_{1/2})$	$V(4p_{1/2})$	$V(4p_{3/2})$	$V(4d_{3/2})$	$V(4d_{5/2})$	$V(4s_{1/2})$	$V(4p_{1/2})$	$V(4p_{3/2})$	$V(4d_{3/2})$	$V(4d_{5/2})$
	SE					UP				
$1s_{1/2}$	348.231	348.232	348.248	348.260	348.260	-91.766	-91.767	-91.771	-91.774	-91.774
$2s_{1/2}$	58.108	58.103	58.108	58.113	58.116	-14.622	-14.620	-14.622	-14.623	-14.624
$2p_{1/2}$	7.671	7.670	7.671	7.674	7.675	-2.383	-2.382	-2.383	-2.384	-2.384
$2p_{3/2}$	7.137	7.136	7.137	7.139	7.140	-0.080	-0.080	-0.080	-0.080	-0.080
$3s_{1/2}$	14.347	14.344	14.349	14.345	14.346	-3.577	-3.576	-3.577	-3.576	-3.577
$3p_{1/2}$	2.269	2.268	2.269	2.269	2.269	-0.658	-0.658	-0.658	-0.658	-0.658
$3p_{3/2}$	1.966	1.965	1.966	1.966	1.966	-0.025	-0.025	-0.025	-0.025	-0.025
$3d_{3/2}$	-0.172	-0.172	-0.172	-0.172	-0.172	0.003	0.003	0.003	0.003	0.003
$3d_{5/2}$	0.245	0.245	0.245	0.245	0.245	0.003	0.003	0.003	0.003	0.003
$4s_{1/2}$	5.079	5.078	5.080	5.079	5.079	-1.263	-1.263	-1.263	-1.263	-1.263
$4p_{1/2}$	0.837	0.837	0.837	0.837	0.837	-0.239	-0.239	-0.239	-0.239	-0.239
$4p_{3/2}$	0.749	0.749	0.749	0.749	0.749	-0.010	-0.010	-0.010	-0.010	-0.010
$4d_{3/2}$	-0.045	-0.045	-0.045	-0.045	-0.045	0.001	0.001	0.001	0.001	0.001
$4d_{5/2}$	0.103	0.103	0.103	0.103	0.103	0.001	0.001	0.001	0.001	0.001
	WK					QED				
$1s_{1/2}$	4.878	4.878	4.879	4.879	4.879	261.344	261.344	261.356	261.365	261.365
$2s_{1/2}$	0.730	0.730	0.730	0.730	0.730	44.216	44.212	44.216	44.220	44.223
$2p_{1/2}$	0.170	0.170	0.170	0.170	0.170	5.459	5.458	5.459	5.461	5.461
$2p_{3/2}$	0.018	0.018	0.018	0.018	0.018	7.075	7.073	7.075	7.076	7.077
$3s_{1/2}$	0.177	0.177	0.177	0.177	0.177	10.947	10.945	10.948	10.945	10.946
$3p_{1/2}$	0.046	0.046	0.046	0.046	0.046	1.657	1.656	1.657	1.657	1.657
$3p_{3/2}$	0.005	0.005	0.005	0.005	0.005	1.946	1.945	1.946	1.946	1.946
$3d_{3/2}$	0.000	0.000	0.000	0.000	0.000	-0.169	-0.169	-0.169	-0.169	-0.169
$3d_{5/2}$	0.000	0.000	0.000	0.000	0.000	0.248	0.248	0.248	0.248	0.248
$4s_{1/2}$	0.062	0.062	0.062	0.062	0.062	3.879	3.878	3.879	3.878	3.879
$4p_{1/2}$	0.017	0.017	0.017	0.017	0.017	0.615	0.615	0.615	0.615	0.615
$4p_{3/2}$	0.002	0.002	0.002	0.002	0.002	0.741	0.741	0.741	0.741	0.741
$4d_{3/2}$	0.000	0.000	0.000	0.000	0.000	-0.044	-0.044	-0.044	-0.044	-0.044
$4d_{5/2}$	0.000	0.000	0.000	0.000	0.000	0.104	0.104	0.104	0.104	0.104

TABLE II: Core relaxation and valence electron contributions to QED corrections (eV) of the $4s-4p$ and $4p-4d$ transitions in Cu-like uranium.

	$4s_{1/2}-$ $4p_{1/2}$	$4s_{1/2}-$ $4p_{3/2}$	$4p_{1/2}-$ $4d_{3/2}$	$4p_{3/2}-$ $4d_{3/2}$	$4p_{3/2}-$ $4d_{5/2}$	$4s_{1/2}-$ $4p_{1/2}$	$4s_{1/2}-$ $4p_{3/2}$	$4p_{1/2}-$ $4d_{3/2}$	$4p_{3/2}-$ $4d_{3/2}$	$4p_{3/2}-$ $4d_{5/2}$
	SE					UP				
$1s_{1/2}$	0.002	0.033	0.055	0.024	0.025	-0.001	-0.010	-0.015	-0.006	-0.006
$2s_{1/2}$	-0.010	0.000	0.021	0.011	0.017	0.002	0.000	-0.006	-0.003	-0.004
$2p_{1/2}$	-0.003	0.000	0.009	0.006	0.007	0.001	0.000	-0.003	-0.002	-0.002
$2p_{3/2}$	-0.006	-0.001	0.012	0.007	0.010	0.000	0.000	0.000	0.000	0.000
$3s_{1/2}$	-0.006	0.004	0.002	-0.008	-0.005	0.001	-0.001	-0.001	0.002	0.001
$3p_{1/2}$	-0.001	0.001	0.001	-0.001	0.000	0.000	0.000	0.000	0.000	0.000
$3p_{3/2}$	-0.003	0.002	0.002	-0.002	-0.001	0.000	0.000	0.000	0.000	0.000
$3d_{3/2}$	0.000	0.000	0.000	0.000	0.000	0.000	0.000	0.000	0.000	0.000
$3d_{5/2}$	-0.001	0.000	0.000	-0.002	-0.001	0.000	0.000	0.000	0.000	0.000
ΔE_{relax}	-0.028	0.040	0.103	0.036	0.051	0.004	-0.012	-0.024	-0.009	-0.012
$\Delta E_{valence}$	-4.242	-4.330	-0.881	-0.794	-0.646	1.024	1.253	0.239	0.011	0.011
ΔE_{QED}	-4.270	-4.290	-0.778	-0.758	-0.595	1.028	1.241	0.215	0.002	-0.001
	WK					QED				
$1s_{1/2}$	0.000	0.000	0.000	0.000	0.000	0.001	0.023	0.040	0.018	0.018
$2s_{1/2}$	0.000	0.000	0.000	0.000	0.000	-0.007	0.000	0.015	0.008	0.013
$2p_{1/2}$	0.000	0.000	0.000	0.000	0.000	-0.002	0.000	0.007	0.004	0.005
$2p_{3/2}$	0.000	0.000	0.000	0.000	0.000	-0.006	-0.001	0.012	0.007	0.010
$3s_{1/2}$	0.000	0.000	0.000	0.000	0.000	-0.004	0.003	0.001	-0.006	-0.004
$3p_{1/2}$	0.000	0.000	0.000	0.000	0.000	-0.001	0.001	0.001	-0.001	0.000
$3p_{3/2}$	0.000	0.000	0.000	0.000	0.000	-0.003	0.002	0.002	-0.002	-0.001
$3d_{3/2}$	0.000	0.000	0.000	0.000	0.000	0.000	0.000	0.000	0.000	0.000
$3d_{5/2}$	0.000	0.000	0.000	0.000	0.000	-0.001	0.000	0.000	-0.002	-0.001
ΔE_{relax}	0.000	0.000	0.000	0.000	0.000	-0.024	0.028	0.079	0.027	0.039
$\Delta E_{valence}$	-0.046	-0.060	-0.016	-0.002	-0.002	-3.264	-3.137	-0.659	-0.785	-0.638
ΔE_{QED}	-0.046	-0.060	-0.016	-0.002	-0.002	-3.288	-3.109	-0.580	-0.758	-0.598

TABLE III: The $4s-4p$ transition energies (eV) of Cu-like ions.

Contribution		Yb^{41+}	W^{45+}	Os^{46+}	Au^{50+}	Pb^{53+}	Bi^{54+}	Th^{61+}	U^{63+}
					$4s_{1/2}-4p_{1/2}$				
RMBPT	Coulomb	88.21	97.85	102.82	110.49	118.42	121.12	140.85	146.75
	Breit	0.83	1.06	1.19	1.40	1.65	1.74	2.47	2.72
	Sum	89.04(2)	98.90(2)	104.01(2)	111.89(2)	120.07(2)	122.86(2)	143.31(2)	149.47(2)
	RMBPT-90[a]	89.02	98.89		111.88	120.05	122.84	143.35	149.45
	RCI[b]		98.90		111.89	120.07		143.31	149.46
QED	SE	−1.28	−1.64	−1.84	−2.18	−2.56	−2.70	−3.85	−4.24
	UP	0.21	0.29	0.33	0.42	0.52	0.55	0.90	1.02
	WK	−0.01	−0.01	−0.01	−0.02	−0.02	−0.02	−0.04	−0.05
	Relax	0.00	−0.01	−0.01	−0.01	−0.01	−0.01	−0.02	−0.02
	2-loop	0.00	0.00	0.01	0.01	0.01	0.01	0.02	0.02
	Sum	−1.08(4)	−1.36(4)	−1.52(4)	−1.78(4)	−2.07(4)	−2.17(4)	−3.00(4)	−3.27(4)
Theory		87.96(4)	97.54(4)	102.49(4)	110.11(4)	118.00(4)	120.68(4)	140.31(4)	146.20(4)
Expt[c]						118.010(1)			
					$4s_{1/2}-4p_{3/2}$				
RMBPT	Coulomb	164.48	200.25	220.75	255.23	294.77	309.19	430.72	473.13
	Breit	−0.08	−0.14	−0.17	−0.24	−0.33	−0.37	−0.71	−0.85
	Sum	164.40(2)	200.12(2)	220.58(2)	254.99(2)	294.43(2)	308.82(2)	430.00(2)	472.28(2)
	RMBPT-90[a]	164.39	200.11		254.98	294.43	308.81	430.05	472.27
	RCI[b]		200.13		255.01	294.45		430.03	472.30
QED	SE	−1.21	−1.56	−1.76	−2.10	−2.50	−2.64	−3.89	−4.33
	UP	0.23	0.32	0.37	0.47	0.60	0.64	1.08	1.25
	WK	−0.01	−0.01	−0.01	−0.02	−0.02	−0.03	−0.05	−0.06
	Relax	0.01	0.01	0.01	0.01	0.01	0.01	0.02	0.03
	2-loop	0.00	0.00	0.01	0.01	0.01	0.01	0.02	0.02
	Sum	−0.98(4)	−1.24(4)	−1.39(4)	−1.63(4)	−1.91(4)	−2.01(4)	−2.82(4)	−3.09(4)
Theory		163.42(4)	198.88(4)	219.19(4)	253.36(4)	292.53(4)	306.82(4)	427.19(4)	469.19(4)
Expt	EBIT-03[d]	163.44(1)	198.90(1)		253.40(1)	292.59(4)			
	EBIT-04[e]			219.20(1)			306.84(2)	427.20(1)	469.22(3)

[a]Ref. [8]
[b]Ref. [9]
[c]Ref. [24]
[d]Ref. [25]
[e]Ref. [26]

TABLE IV: The $4p-4d$ transition energies (eV) of Cu-like ions.

Contribution		Yb^{41+}	W^{45+}	Os^{46+}	Au^{50+}	Pb^{53+}	Bi^{54+}	Th^{61+}	U^{63+}
					$4p_{1/2}-4d_{3/2}$				
RMBPT	Coulomb	214.22	253.62	275.84	312.78	354.64	369.81	496.14	539.81
	Breit	−1.26	−1.59	−1.78	−2.10	−2.46	−2.60	−3.72	−4.12
	Sum	212.96(2)	252.03(2)	274.06(2)	310.68(2)	352.18(2)	367.21(2)	492.42(2)	535.69(2)
QED	SE	−0.11	−0.17	−0.20	−0.28	−0.37	−0.40	−0.74	−0.88
	UP	0.02	0.03	0.04	0.06	0.08	0.09	0.19	0.24
	WK	0.00	0.00	0.00	0.00	0.00	−0.01	−0.01	−0.02
	Relax	0.02	0.03	0.03	0.04	0.04	0.05	0.07	0.08
	Sum	−0.07(4)	−0.11(4)	−0.13(4)	−0.18(4)	−0.24(4)	−0.27(4)	−0.49(4)	−0.58(4)
Theory		212.89(4)	251.92(4)	273.92(4)	310.50(4)	351.93(4)	366.94(4)	491.93(4)	535.11(4)
Expt[a]							366.97(2)	491.94(10)	535.15(5)
					$4p_{3/2}-4d_{3/2}$				
RMBPT	Coulomb	137.95	151.21	157.91	168.04	178.29	181.74	206.27	213.42
	Breit	−0.35	−0.40	−0.42	−0.45	−0.48	−0.49	−0.54	−0.55
	Sum	137.60(2)	150.81(2)	157.49(2)	167.59(2)	177.81(2)	181.24(2)	205.73(2)	212.87(2)
QED	SE	−0.18	−0.25	−0.28	−0.35	−0.43	−0.46	−0.71	−0.79
	UP	0.00	0.00	0.00	0.00	0.00	0.01	0.01	0.01
	WK	0.00	0.00	0.00	0.00	0.00	0.00	0.00	0.00
	Relax	0.01	0.01	0.02	0.02	0.02	0.02	0.03	0.03
	Sum	−0.17(4)	−0.23(4)	−0.27(4)	−0.33(4)	−0.41(4)	−0.43(4)	−0.67(4)	−0.76(4)
Theory		137.43(4)	150.58(4)	157.22(4)	167.26(4)	177.40(4)	180.81(4)	205.05(4)	212.12(4)
					$4p_{3/2}-4d_{5/2}$				
RMBPT	Coulomb	154.35	173.27	187.19	199.10	215.94	221.80	266.72	280.93
	Breit	−0.74	−0.89	−0.98	−1.11	−1.25	−1.30	−1.66	−1.77
	Sum	153.61(2)	172.37(2)	186.21(2)	197.99(2)	214.69(2)	220.50(2)	265.05(2)	279.16(2)
QED	SE	−0.14	−0.19	−0.22	−0.28	−0.34	−0.37	−0.57	−0.65
	UP	0.00	0.00	0.00	0.00	0.00	0.01	0.01	0.01
	WK	0.00	0.00	0.00	0.00	0.00	0.00	0.00	0.00
	Relax	0.01	0.02	0.02	0.02	0.03	0.03	0.04	0.04
	Sum	−0.13(4)	−0.17(4)	−0.20(4)	−0.25(4)	−0.31(4)	−0.34(4)	−0.53(4)	−0.60(4)
Theory		153.48(4)	172.20(4)	186.00(4)	197.74(4)	214.38(4)	220.17(4)	264.52(4)	278.56(4)

[a]Ref. [4]

TABLE V: QED energies (eV) for the $4l - 4l'$ transitions in Cu-like ions. $\Delta E_{valence}$ and ΔE_{QED} are frozen-core and relaxed-core results of this work. References to the empirical data can be found in Tables III and IV.

Z	$\Delta E_{valence}$	ΔE_{QED}	Blundell[a]	Kim *et. al.*[b]	Empirical
			$4s_{1/2} - 4p_{1/2}$		
70	−1.07	−1.08(4)	−1.06	−1.06	
74	−1.35	−1.36(4)	−1.34	−1.33	
76	−1.51	−1.52(4)		−1.48	
79	−1.77	−1.78(4)		−1.74	
82	−2.06	−2.07(4)	−2.05	−2.02	−2.05(2)
83	−2.16	−2.17(4)	−2.15	−2.12	
90	−2.98	−3.00(4)	−2.98	−2.92	
92	−3.25	−3.27(4)	−3.25	−3.18	
			$4s_{1/2} - 4p_{3/2}$		
70	−0.98	−0.98(4)	−0.96	−0.96	−0.96(2)
74	−1.25	−1.24(4)	−1.22	−1.21	−1.22(2)
76	−1.39	−1.39(4)		−1.35	−1.38(2)
79	−1.64	−1.63(4)		−1.59	−1.59(2)
82	−1.92	−1.91(4)	−1.88	−1.86	−1.84(4)
83	−2.02	−2.01(4)	−1.98	−1.95	−1.98(3)
90	−2.84	−2.82(4)	−2.78	−2.73	−2.81(2)
92	−3.12	−3.09(4)	−3.05	−2.99	−3.06(3)
			$4p_{1/2} - 4d_{3/2}$		
70	−0.09	−0.07(4)			
74	−0.14	−0.11(4)			
76	−0.16	−0.13(4)			
79	−0.22	−0.18(4)			
82	−0.29	−0.24(4)			
83	−0.31	−0.27(4)			−0.24(3)
90	−0.56	−0.49(4)			−0.48(10)
92	−0.66	−0.58(4)			−0.54(5)

[a]Ref. [11]

[b]Ref. [10]